Ab Initio Study of Proton Transfer between Protonated Formohydroxamic Acid and Water Molecules

Szu-Jen Yen, Ching-Yeh Lin, and Jia-Jen Ho*

Department of Chemistry, National Taiwan Normal University, 88, Section 4, Tingchow Road, Taipei, Taiwan 117, ROC

Received: June 12, 2000; In Final Form: September 29, 2000

Proton transfer between protonated formohydroxamic acid $(FAH)^+$ and water molecules $(H_2O-FAH-H_2O)^+$ is studied theoretically. In a proton-relay mechanism, the carbonyl oxygen in formohydroxamic acid (HCONHOH, FA) accepts a proton from the hydronium ion (H_3O^+) and releases a proton either from the amine group (N−H) or the N-hydroxyl (N−OH) of formohydroxamic acid to another H_2O molecule. The movement of the two protons is not simultaneous but through a stepwise process. The catalytic effect of the H_2O molecule in reducing the proton-transfer barrier compared to the catalytic effect of pure formohydroxamic acid through intramolecular proton transfer is substantial. The transfer barriers of the two protons in a relay process are asymmetric. The proton on either the amine group (N−H) or the N-hydroxyl (N−OH) of FAH^+ will be transferred to the second H_2O molecule, and the proton transfer is determined by the lengths $R_{N\cdots O}$ and $R_{O\cdots O}$, which are related to the distance between FAH^+ and the second H_2O molecule. At the same $R_{N\cdots O}$ and $R_{O\cdots O}$, the proton on amino group (N−H) has a transfer energy barrier lower than that of the proton on the N-hydroxyl site by about 4.1 kcal/mol. If we elongate the distance between the two water molecules and let protonated FA shuttle freely as a proton carrier between the two water molecules, then the energy barrier for the movement of protonated FA increases slowly with the increase of the distance between two H_2O's separated by no more than 10 Å. However, the proton-transfer barrier between protonated FA and water is independent of the separated distance of the two water molecules.

Introduction

Scheiner et al.[1,2] has studied theoretically the proton transfer between molecules containing oxygen atoms, such as $(H_2O-H-OH_2)^+$, $(H_2O-H-OCH_2)^+$, and $(H_2O-H-O(OH)CH)^+$. They also compared the transfer barriers with some more complicated systems containing oxygen and nitrogen atoms,[3] such as $(H_2O-H-NH_3)^+$, $(H_2O-H-NH_2CHO)^+$, etc. Since proton transfer frequently occurred in biochemical systems, especially between proteins, we chose formohydroxamic acid (FA) to mimic the simplest structure (NH···O═C) in the protein α-helix skeleton and studied theoretically the proton-transfer characters. Water molecule plays an important role in most of the chemical reactions and was widely used as a solvent in the reaction. In this paper, we added two H_2O molecules around the protonated formohydroxamic acid $(FAH)^+$ and studied the inter- and intramolecular proton-transfer potential profile in the $(H_2O-FAH-H_2O)^+$ complex system. The formohydroxamic acid molecule contains hydroxyl, carbonyl, and amino functional groups. Therefore, it acts not only as a weak acid but also as a weak base. We let FA accept a proton at the carbonyl site of the structure from a hydronium ion and release the proton at other via intramolecular proton transfer. Two proton transfers are involved. They may be carried out through concerted or stepwise processes.

Several studies were carried out to determine which proton (N−H or N−OH) of hydroxamic acids is being transferred in the tautomeric processes. Gal et al.[5] measured the gas-phase activities of acetohydroxamic acid and its O-methyl and N-methyl derivatives, concluding that it behaves essentially as an N-acid in the gas phase. Theoretical calculations in the literature[6] showed that both formo- and acetohydroxamic acids should behave as N-acids in gas phase but O-acids in aqueous solution. The results for DMSO solution are not conclusive. Our recent calculation[4] also showed that formohydroxamic acid should act as an N-acid in the gas phase. Bagno et al.,[7] from their hetronuclear (^{14}N, ^{15}N, and ^{17}O) relaxation time measurement, indicated that in aqueous solution acetohydroxamic acid is predominately an O-acid, whereas benzohydroxamic acid is predominately an N-acid. In this paper, we use two H_2O molecules along with the protonated formohydroxamic acid FAH^+ to simulate the inter- and intramolecular proton transfers in $(H_2O-FAH-H_2O)^+$. The result may provide answers to the proportion of N-acid or O-acid of formohydroxamic acid in the surrounding water molecules.

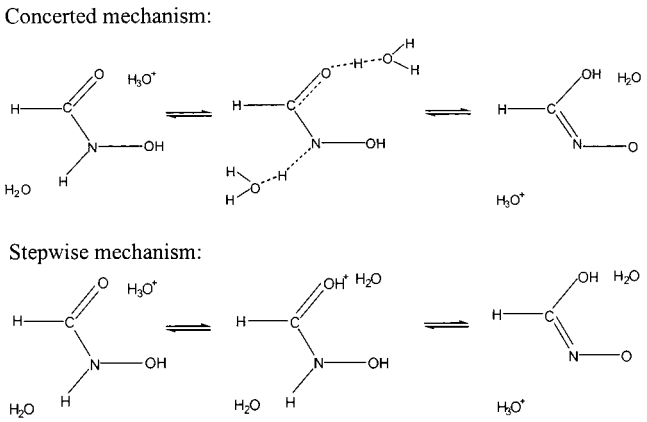

* Corresponding author. Phone: (886)-2-29309085. Fax: (886)-2-29324249. E-mail: jjh@scc.ntnu.edu.tw.

10.1021/jp0021143 CCC: $19.00
Published on Web 11/23/2000

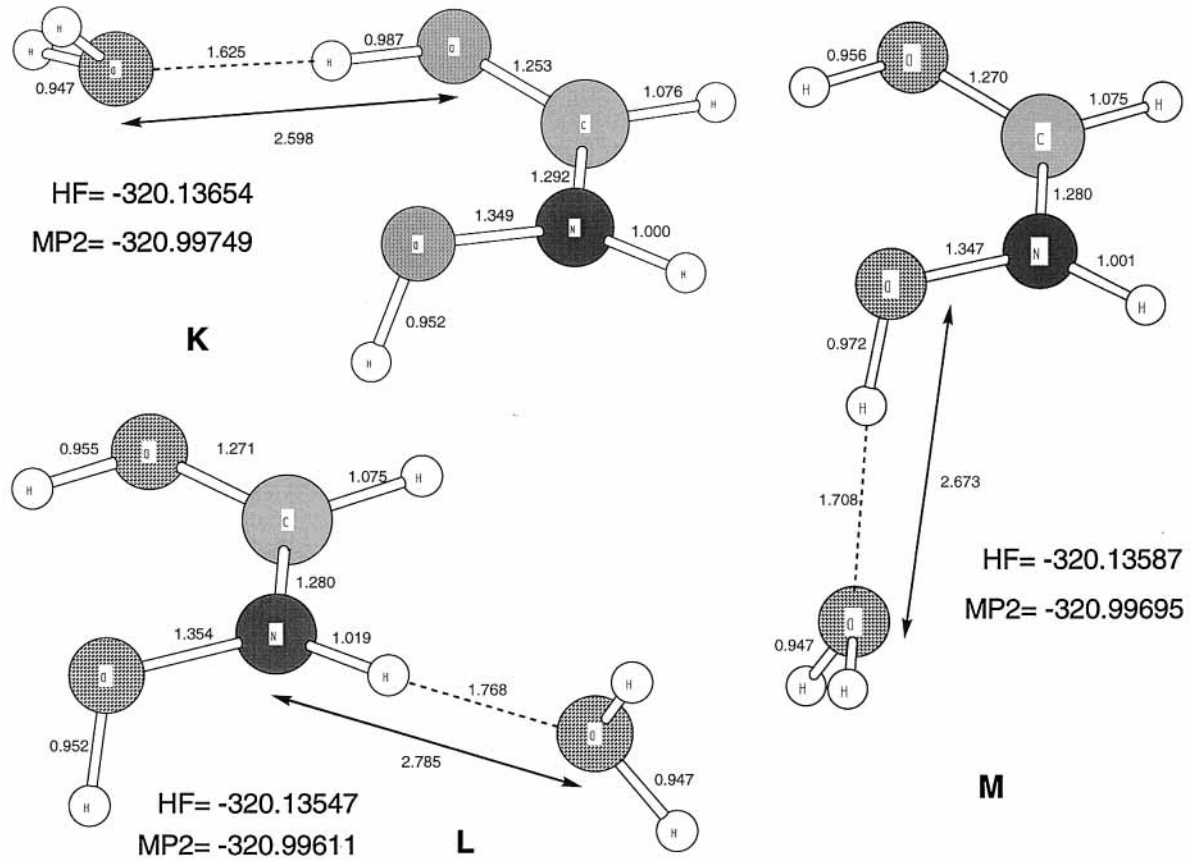

Figure 1. Optimized geometries of a protonated formohydroxamic acid−water complex. There are three different positions for the water molecule around the protonated formohydroxamic acid. They are labeled K, L, and M. The HF and MP2 energies are in au and the bond lengths in Å

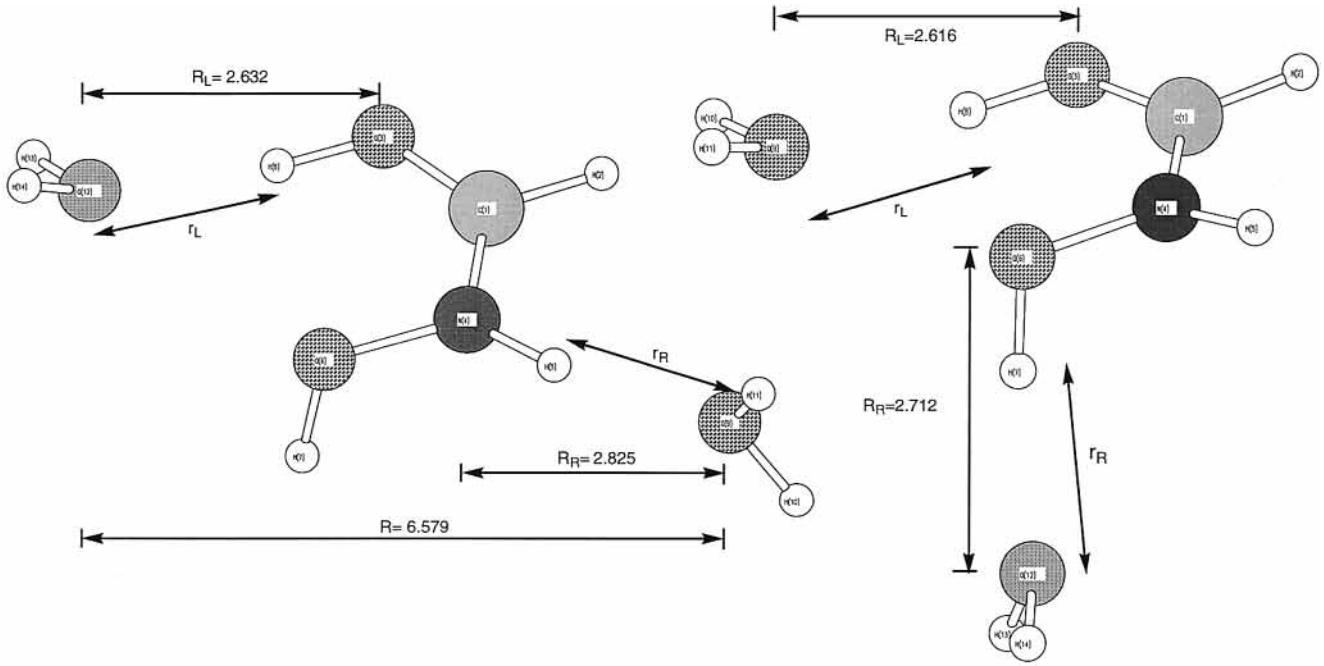

Figure 2. Optimized geometries of $(H_2O-FAH-H_2O)^+$. The second H_2O is placed around the N−H site (left graph) or the N−OH site (right graph). They were obtained without any prior assumption concerning their symmetry. All parameters were fully optimized.

Methods of Calculation. The Gaussian 94 set of ab initio computer codes[8] was employed for all calculations. The geometries of protonated formohydroxamic acid $(FAH)^+$ with a neutral H_2O molecule were first optimized with the gradient schemes included in the program package. The H_2O molecule was placed around the three functional groups (carbonyl, hydroxyl, and amino) of the FAH^+ (see Figure 1) to calculate the proton-transfer barriers. To create a double-well potential, we extended the heavy-atom distance $R(O_{FAH}-O_{H2O})$ a small amount over the equilibrium distance. The second H_2O molecule was then added, $(H_2O\cdots FAH\cdots H_2O)^+$ (see Figure 2), and the optimized complex structures were calculated. $R_L(O-O)$ and $R_R(O-O)$ (the distances between the two heavy atoms to the left and right, respectively, of the FA molecule) were chosen

TABLE 1: Binding Energies[a] of (H_2O-FAH^+) Complexes (kcal/mol)

species	HF[b]	MP2[c]
K	19.2	22.3
L	18.5	21.4
M	18.7	21.9

[a] Binding energy = $E(FAH^+) + E(H_2O) - E(FAH^+\cdots H_2O)$. [b] Calculated with fully optimized methods in the 6-31+G** basis set. [c] Energies calculated at MP2/6-31+G**//HF/6-31+G**.

for several distances, the values of r_L and r_R were varied, and the potential profile of proton transfer was then obtained. This model could be considered as a combination of the formohydroxamic acid (as a peptide) and a pair of water molecules all situated within a protein and should thereby be subject to constraints that prevent the molecules from approaching to their optimal distance. Finally, the two H_2O molecules were placed 10 Å away, and the FA molecule was positioned near the first protonated H_2O molecule. After accepting the proton from the H_3O^+ ion, FAH^+ acts as a proton carrier to shuttle between the two separated water molecules and eventually transfers the proton to the second H_2O molecule. The potential energy profile was then calculated. This process was to examine the shuttling capacity of the formohydroxamic acid species. The polarized split valence basis set with the diffuse function, 6-31+G**, was used because Wiberg[9] had verified that this basis set yielded satisfactory agreement with experiments in his formic acid calculation. For single-point energy calculation, MP2/6-31+G**//HF/6-31+G** was employed for the complex systems of $(H_2O\cdot\cdot\cdot FAH\cdots OH_2)^+$.

Results and Discussion

The optimized structures of protonated formohydroxamic acid combined with one water molecule ($HFA^+\cdots H_2O$) at three different possible sites are plotted in Figure 1, labeled as K, L, and M. The calculated binding energy of the complex molecule is listed in Table 1. Since the geometry of protonated formohydroxamic acid (HFA^+) does not change significantly from that of FA, the factors that determine the magnitude of the binding energy of the $(H_2O-HFA)^+$ complex are the strength of the hydrogen bonding (N−H···O or O−H···O) and the distance between the two heavy atoms. As the oxygen atom has larger electron negativity, the hydrogen bonding strength of O−H···O is greater than that of N−H···O, and the distance between the two heavy atoms in structure K is the smallest (2.598 Å). Accordingly, the calculated binding energy follows the order K > M > L. Now we add another H_2O molecule around the $(HFA-H_2O)^+$ complex and model the possible proton-transfer processes among these three molecules. From theoretical studies,[10,11] the best possible site of protonation on FA is the carbonyl oxygen. Therefore, we first put the hydronium ion (H_3O^+), the proton donor, around the carbonyl group of FA and let the carbonyl oxygen accept the proton from the hydronium ion. The second H_2O molecule acts as a proton acceptor, which may accept the proton from the protonated FA. There are two sites in the FAH that may release the proton. One is from the amine group (N−H) and the other the N-hydroxyl group (N−OH). We added the second H_2O molecule around these two sites separately and studied theoretically the difference of the potential profiles of proton transfer in these two circumstances.

1. Placing the Second H_2O around the Amine Group (N−H). The fully optimized $(H_2O-HFA-H_2O)^+$ complex is shown in Figure 2. The calculated equilibrium length of R_L and R_R (the distances between the two heavy H_2O molecules to the left and right, respectively, of the FA molecule) is 2.632 and 2.825 Å, respectively. To obtain a double-well potential, we extended R_R and R_L accordingly. The transfer potential profile was then

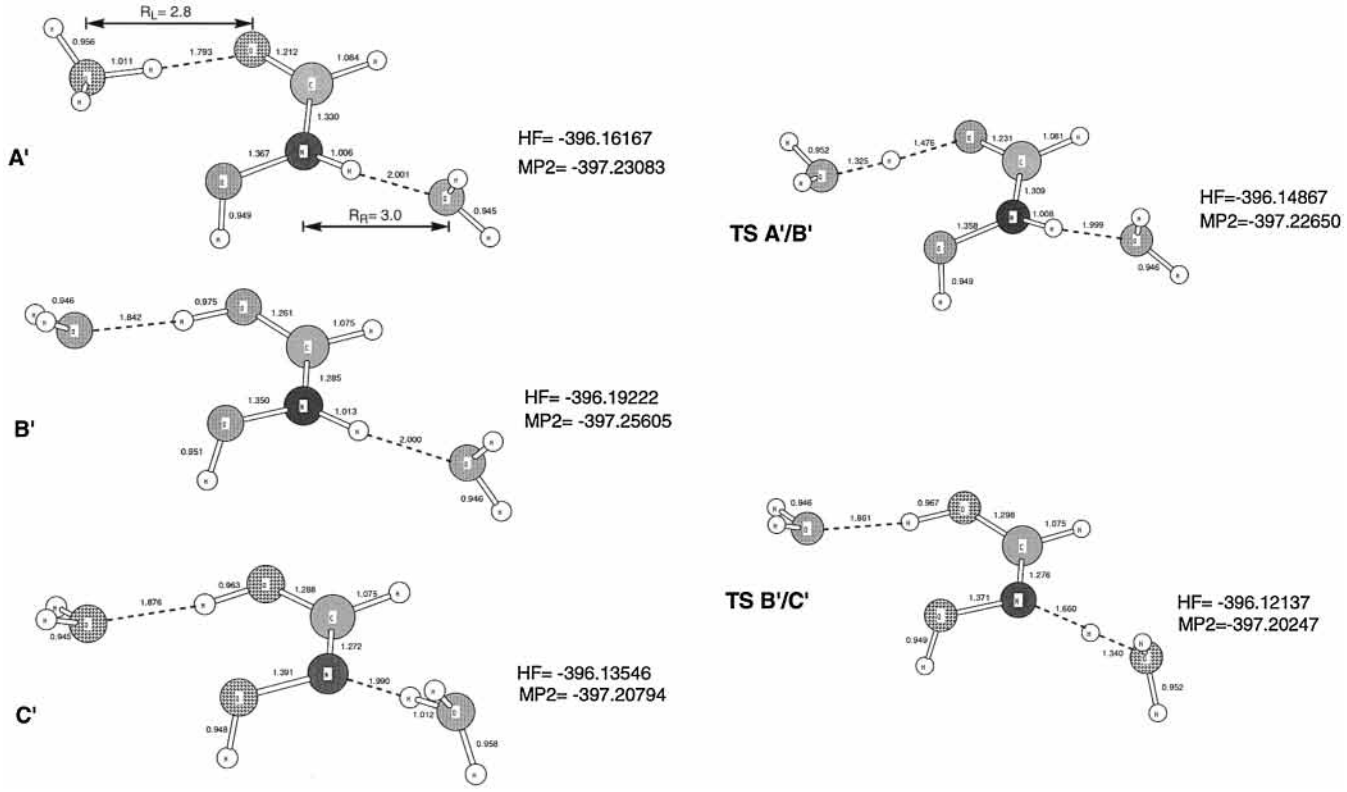

Figure 3. Optimized geometries of A′, B′, C′, and their corresponding transition state structures TSA′/B′, TSB′/C′. R_L and R_R are kept at 2.800 and 3.000 Å, respectively, when proton transfer proceeds. The HF and MP2 energies are given in au and the bond lengths in Å.

TABLE 2: Calculated Relative Energies of the Protonated ($H_2O\cdots FA\cdots H_2O$) Complexes and Their Corresponding Transition State Structures (in kcal/mol)

	species	HF[d]	MP2[e]
	A′	19.2	15.8
	TSA′/B′	27.3	18.5
I[a]	B′	0.0	0.0
	TSB′/C′	44.5	33.6
	C′	35.6	30.2
	A″	18.8	15.5
	TSA″/B″	27.1	18.3
II[b]	B"	0.0	0.0
	TSB″/C″	52.9	40.6
	C″	37.8	32.5
	D′	16.9	13.6
	TSD′/E′	26.1	17.3
III[c]	E′	0.0	0.0
	TSE′/F′	52.0	37.7
	F′	42.1	34.0

[a] Energies are reported with respect to B′ when $R_L = 2.800$ Å and $R_R = 3.000$ Å. [b] Energies are reported with respect to B″ when $R_L = 2.800$ Å and $R_R = 3.125$ Å. [c] Energies are reported with respect to E′ when $R_L = 2.800$ Å and $R_R = 3.000$ Å. [d] Calculated with fully optimized methods in the 6-31+G** basis set. [e] Energies calculated at MP2/6-31+G**//HF/6-31+G**.

TABLE 3: Proton-Transfer Barriers in ($FAH^+\cdots H_2O$) and ($H_2O\cdots FAH^+\cdots H_2O$) Systems

	1 $FAH^+ \rightarrow OH_2$[a]		2 $FA \leftarrow H^+OH_2$[b]	
	HF[c]	MP2[d]	HF[c]	MP2[d]
K′ [e]	25.0	16.4	9.6	4.1
L′ [f]	40.8	29.9	10.9	5.5
M′ [g]	48.4	34.2	12.4	5.6
	3 $H_2O\cdots FAH^+ \rightarrow OH_2$[a]		4 $H_2O\cdots FA \leftarrow H^+OH_2$[b]	
	HF[c]	MP2[d]	HF[c]	MP2[d]
$K' + H_2O$[h]	27.3	18.5	8.1	2.7
$K' + H_2O$[i]	26.1	17.3	9.2	3.7
$L' + H_2O$[j]	44.5	33.6	8.9	3.4
$M' + H_2O$[k]	52.0	37.7	9.9	3.7

[a] Proton transfer from formohydroxamic acid to water. [b] Proton transfer from water to formohydroxamic acid. [c] Calculated with fully optimized methods in the 6-31+G** basis set. [d] Energies calculated at MP2/6-31+G**//HF/6-31+G**. [e] The geometry structure resembles K, but R(O···O) = 2.800 Å. [f] The geometry structure resembles L, but R(N···O) = 3.000 Å. [g] The geometry structure resembles M, but R(O···O) = 3.000 Å. [h] The second water is added near the amino group, and R(N···O) = 3.000 Å. [i] The second water is added near the hydroxyl group, and R(O···O) = 3.000 Å. [j] The second water is added near the carbonyl group, and R(O···O) = 2.800 Å. [k] The second water is added near the carbonyl group, and R(O···O) = 2.800 Å.

calculated by changing r_L and r_R separately and the transition state obtained. As illustrated in Figure 3, the transfer of proton started from the local minimum A′, where the proton was first attached to the left H_2O molecule, to the transition state, TSA′/B′, and then to another local minimum B′, where the proton was transferred to the FA molecule. The length of N−H bond in HFA^+ did not elongate during the transfer process (A′ → TSA′/B′). This implied that the proton transfer in this triad preferred a stepwise process. This result was similar to the system of (NH_3−protonated imidazole−NH_3)$^+$ from Scheiner[12] and by Nagaoka[13] in keto−enol tautomeric system. The release of the proton to the other H_2O molecule was then followed from B′ to the transition state TSB′/C′ and to then C′. It completed the proton transfer $H_3O^+ \rightarrow FA \rightarrow H_2O$. The calculated relative energies of all the species on the potential profile are listed in Table 2. The results of $R_L = 2.800$ Å, $R_R = 3.000$ Å and $R_L = 2.800$ Å, $R_R = 3.125$ Å are listed in cases I and II of the table, and the corresponding structures are denoted as A′, B′, C′ and A″, B″, C″, respectively. The basic structures in case II are analogous to those shown in Figure 3, except that the R_R in each structure is kept at 3.125 Å. The transfer process from A′ to C′ turns the FA molecule from the keto to the iminol form. However, the total energy barrier via this process is equal to the difference of the relative energies between TSB′/C′ and A′. It is only 17.8 kcal/mol (MP2 of Table 2I), much smaller than the analogous conversion of FA through intramolecular hydrogen transfer (46.1 kcal/mol)[4] without any assistance of H_2O molecules. Clearly, the catalytic effect of H_2O molecules is significant. The elongation of R_R from 3.000 to 3.125 Å in case II of the table increases the barrier to 25.1 kcal/mol. The distance of R_R (on the condition of fixed R_L) is crucial to the total energy barrier in this two-proton transfer process.

2. Placing the Second H_2O around the N-Hydroxyl Group (N−OH). The optimized structure in this configuration is shown in the right part of Figure 2. The calculated equilibrium distances

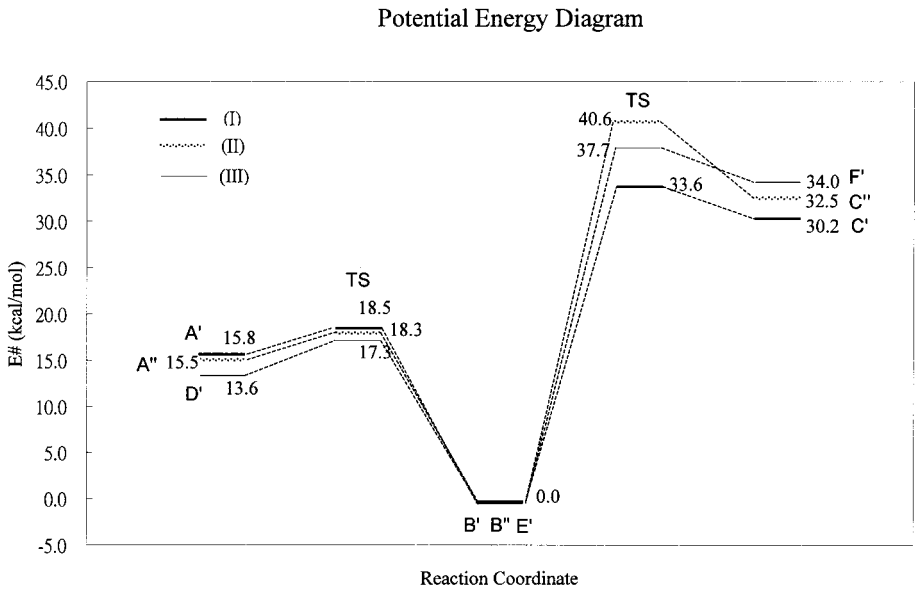

Figure 4. Schematic diagram of the relative energies for the species list in I, II, and III of Table 2. Numerical values are given in kcal/mol.

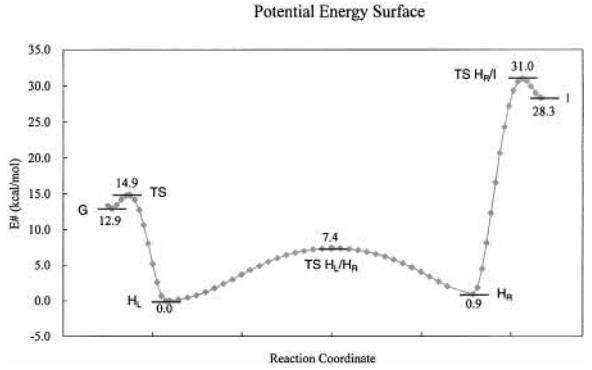

Figure 5. Schematic diagram of the potential energy surfaces describing proton transfer from triads of $(H_3O-FA-H_2O)^+$ (G) to H_L, H_R, and then $(H_2O-FA-H_3O)^+$ (I). The separation of two H_2O molecules is set at 10 Å.

between the two heavy atoms, R_L and R_R, are slightly longer when compared to those of the $(H_3O-FA)^+$ and $(FAH-H_2O)^+$ diads (in Figure 1; $R_L = 2.616$ and 2.598 Å and $R_R = 2.712$ and 2.673 Å). A similar result was also seen in the first circumstance where $R_L = 2.632$ and 2.598 Å and $R_R = 2.825$ and 2.785 Å. The strength of the H-bonding is significantly decreased in $(H_2O-FAH-H_2O)^+$ triads, since the central FAH^+ is acting as the proton donor to both H_2O molecules. In this section, the second H_2O molecule is located right below the FAH to accept the proton as easily as possible. We fixed the equilibrium distances of $R_L = 2.800$ Å and $R_R = 3.000$ Å and performed the proton-transfer calculation to obtain the transfer potential profile. The geometric structures for sequential steps of proton transfer labeled D′, TSD′/E′, E′, TSE′/F′, and F′ are analogous to the corresponding steps in Figure 3, except the second H_2O is positioned around the N−OH site. The transfer processes are also stepwise. However, in the change of geometries (E′ → TSE′/F′ → F′), the second H_2O has a tendency to move toward the first H_2O molecule to form hydrogen bonding. The calculated result was listed in Table 2III. The calculated reaction energies of A′ → TSA′/B′ → B′ → ... C′ in case I of the table is +14.4 kcal/mol (MP2, the difference between C′ and A′), which is smaller than the 20.4 kcal/mol of the reaction (D′ → TSD′/E′ → ... F′) in case III of the table. Thermodynamically, process I is more favored than III. The energy barriers for process I, II, and III are also plotted in Figure 4. The major barriers in I and III are from B′ → C′ (33.6 kcal/mol) and E′ → F′ (37.7 kcal/mol), respectively, where R_L and R_R are equal to 2.800 and 3.000 Å in both processes I and III. Therefore, kinetically, process I is also more favored. That is, if the proton transfer were designed in the $(H_3O-FA-H_2O)^+$ triad, the second H_2O molecule acting as the proton acceptor prefer to be located around the amine site (N−H group). The R_R values in calculations for both I and III were fixed at 3.000 Å. However, the R_R in I represents the distance between N and O atoms and that in III the distance between O and O atoms. In general, these R_R values in two cases should be different at the equilibrium structures, since the interaction forces between N···O and O···O are different. The calculated equilibrium R_R values of $R_{N\cdots O}$ and $R_{O\cdots O}$ for the triads (in Figure 2) are 2.825 and 2.712 Å, respectively. If we elongated the bond distances of these two values with the same ratio instead of the same value, based on $R_{O\cdots O}/R_{O\cdots O} = 2.712:3.0$, then $R_{N\cdots O}/R_{N\cdots O}$ should be 2.825:3.125. The calculated corresponding energies are listed in case II of Table 2 (A″ → TSA″/B″ → B″ → ... C″). The calculated major energy barrier for this process is 40.6 kcal/mol, when R_L and R_R are equal to 2.800 and 3.125 Å, respectively. It implies that process III (37.7 kcal/mol) is more favored kinetically. The second H_2O prefers to be located around

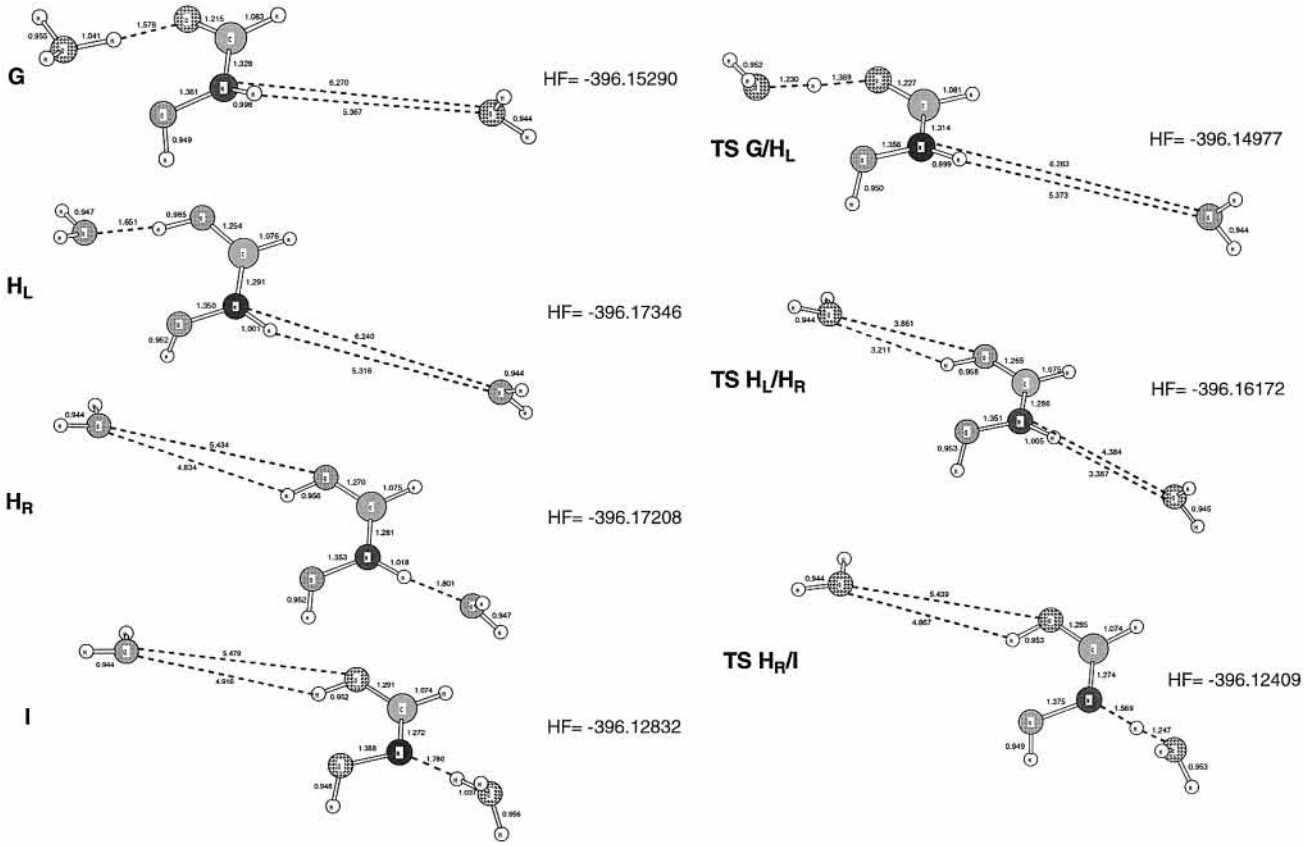

Figure 6. Optimized geometries of G, H_L, H_R, I, and their corresponding transition state structures. The protonated formohydroxamic acid shuttles between the two H_2O molecules separated at 10 Å. The HF energies are in au.

the N-hydroxyl site (N−OH) instead. Therefore, from the comparison of the two sets—I, III and II, III—we know that the R_R value (the distance between FA and the second H_2O molecule) is decisive in determining which proton (N−H or N−OH) is more easily released to the second H_2O in the triad $(H_2O-FAH-H_2O)^+$.

3. Effect of Single-H_2O and Double-H_2O Molecules. We took the data of parts I and III of Table 2 and combined with other data to form Table 3. The upper section of Table 3 shows the proton-transfer barriers in $(FAH \rightarrow H_2O)^+$; the lower section shows the barriers in $(H_2O-FAH-H_2O)^+$. The data under column 4 are all smaller than the corresponding data under column 2, but the data under column 3 are larger than those under column 1. This result shows that the added second H_2O to the system would increase the barrier of proton transfer of the reaction $FAH^+ \rightarrow H_2O$ but decrease the barrier of the $FA \leftarrow H_3O^+$ reaction. These are in good agreement with what Scheiner [12] has done in the $(NH_3\text{-imidozole-}NH_3)^+$ system. The addition of the second H_2O on the other side of FA would increase the basicity of FA and induce a tendency to retain the proton on the central FA. At last we extended the distance between the two H_2O molecules to 10 Å and let FAH^+ act as a proton carrier to shuttle between the molecules. The transfer barriers and corresponding structures were studied. As shown in Figure 5, there are two local minimum structures H_L and H_R, where the energy of H_L is lower than H_R by 0.9 kcal. The geometries of H_L, H_R, and other related structures are plotted in Figure 6. The barrier for FAH^+ to move from the left minimum, H_L, to the right, H_R, is 7.4 kcal/mol. However, the barriers for the FAH^+ to release the proton to the left H_2O to form structure G and the right to form I are different. They are asymmetric ($H_L \rightarrow$ G is 14.9 kcal/mol, $H_R \rightarrow$ I is 30.1 kcal/mol at HF/6-31+G**) and differ from the system of $(NH_3-\text{imidozole}-NH_3)^+$. Imidazole has the same two heavy atoms (nitrogen) in the molecule, while FA molecule has one oxygen at one end and one nitrogen at the other. The barrier for the shuttling of FAH^+ between the two distant H_2O molecules does not vary greatly with respect to the increase of the distance between the two H_2O separated not further than 10 Å. On the contrary, the barrier of proton transfer is sharply increased with the increase of travel distance of proton from FAH^+ to the H_2O.

Conclusion

We have performed the calculation of proton transfer in $(H_2O-FAH-OH_2)^+$ system. The calculated transfer processes and barriers provide some information on the proton transfer in the simple amino acid system with dilute H_2O. The transfer of proton in this system, occurring from one H_2O molecule to FA and then to another H_2O, prefers a stepwise process. In general, the addition of a H_2O molecule to the FA system $(H_2O-FAH)^+$ lowers the intramolecular proton-transfer barriers in a protonated FA system. However, the addition of the second H_2O molecule, $(H_2O-FAH-H_2O)^+$, increases the barrier of transfer process $FAH^+ \rightarrow H_2O$ but decreases in the reverse process $FA \leftarrow H_3O^+$. The proton-transfer barriers are sensitive to the H-bond lengths. In our model, where the combination of formohydroxamic acid (as a peptide) and a pair of water molecules all situated within a protein prevents the molecules from approaching to their optimal distance, we have calculated the following results. When R_L and R_R are equal to 2.800 and 3.000 Å as in I, then the two proton-transfer barriers are 2.7 and 33.6 kcal/mol, respectively. In process II, when R_L and R_R are equal to 2.800 and 3.125 Å, the two proton-transfer barriers are 2.8 and 40.6 kcal/mol, respectively. In process (III) with the second H_2O around the N-hydroxyl group, when R_L and R_R are equal to 2.800 and 3.000 Å, the two proton-transfer barriers are 3.7 and 37.7 kcal/mol, respectively. To determine which proton (from the N−H or N−OH of FA) was transferred to the second H_2O molecule, it is crucial to determine the intermolecular distance between FA and H_2O. We have proved a completely opposite result at two different intermolecular distances.

Acknowledgment. Support for this research from the National Science Council of the Republic of China (NSC-88-2113-M-003-007) is gratefully acknowledged. The authors are also grateful to the National Center for High-Performance Computing, where the Gaussian package and computer time were provided. We are indebted to the reviewers for their helpful suggestions concerning the manuscript.

References and Notes

(1) (a) Scheiner, S. *J. Am. Chem. Soc.* **1981**, *103*, 315. (b) Scheiner, S. *J. Phys. Chem.* **1982**, *86*, 376. (c) Scheiner, S.; Redfern, P.; Szczesniak, M. M. *J. Phys. Chem.* **1985**, *89*, 262.

(2) (a) Scheiner, S.; Hillenbrand, E. A. *J. Phys. Chem.* **1985**, *89*, 3053. (b) Cybulski, S. M.; Scheiner, S. *J. Am. Chem. Soc.* **1989**, *111*, 23.

(3) (a) Scheiner, S. *J. Chem. Phys.* **1982**, *77*, 4039. (b) Scheiner, S.; Harding, L. B. *J. Phys. Chem.* **1983**, *87*, 1145. (c) Scheiner, S.; Wang, L. *J. Am. Chem. Soc.* **1993**, *115*, 1958.

(4) Wu, D. H.; Ho, J. J. *J. Phys. Chem. A* **1998**, *102*, 3582.

(5) Decouzon, M.; Exner, O.; Gal, J.-F.; Maria, P.-C. *J. Org. Chem.* **1990**, *55*, 3980.

(6) Ventura, O. N.; Rama, J. B.; Turi, L.; Dannenberg, J. J. *J. Am. Chem. Soc.* **1993**, *115*, 5754.

(7) Bango, A.; Comuzzi, C.; Scorrano, G. *J. Am. Chem. Soc.* **1994**, *116*, 916.

(8) *Gaussian 94*, Revision B. 3; Gaussian, Inc.: Pittsburgh, PA, 1995.

(9) Wiberg, K. B.; Laidig, K. E. *J. Am. Chem. Soc.* **1987**, *109*, 5935.

(10) Exner, O.; Remko, M.; Mach, P.; Schleyer, P. V. K. *J. Mol. Struct.* (*Theochem*) **1993**, *279*, 139.

(11) Yamin, L. J.; Ponce, C. A.; Estrada, M. R.; Vert, F. T. *J. Mol. Struct.* (*Theochem*) **1996**, *360*, 109.

(12) Scheiner, S.; Yi, M. *J. Phys. Chem.* **1996**, *100*, 9235.

(13) Nagaoka, M.; Suenobu, K.; Yamabe, T. *J. Am. Chem. Soc.* **1997**, *119*, 8023.